

Constraints on possible mechanisms for high- T_c superconductivity

E.Schachinger, I.Schürrer

Institut für Theoretische Physik, Technische Universität Graz,
Petersgasse 16, A-8010 Graz, Austria

Received March 23, 1998

This paper discusses a phenomenological model used to describe various properties of a $d_{x^2-y^2}$ superconductor in its temperature as well as frequency dependence, namely, the London penetration depth, the optical conductivity, the microwave conductivity, and the electronic thermal conductivity. We assume the CuO_2 planes to be the dominant feature for superconductivity and develop a 2D-formalism in which inelastic scattering is modelled explicitly by a spectral density which describes a fluctuation spectrum responsible for the superconducting transition and also for the large inelastic scattering observed in the normal state above the critical temperature T_c . The feedback effect of superconductivity on the spectral density is modelled by a temperature dependent low frequency cutoff. Theoretical results are compared with the experimental data and the fact that such a model allows a consistent description of a variety of phenomena is then used to formulate constraints on possible mechanisms of superconductivity in oxides.

Key words: *high- T_c superconductivity, London penetration depth, optical conductivity, electronic thermal conductivity*

PACS: *74.20.Fg, 74.25.Nf, 74.72.-h*

1. Introduction

Since the discovery of high- T_c superconductivity in oxide materials by Bednorz and Müller [1] huge efforts have been made to find a theoretical description of the pairing mechanism which leads to critical temperatures of the order of 100 K. Nevertheless, it is only recently that a consistent set of experiments performed on high quality twinned and untwinned single crystals of optimally doped $\text{YBa}_2\text{Cu}_3\text{O}_{6.95}$ (YBCO) seem to have resolved the symmetry of the superconducting order parameter to be predominantly of the $d_{x^2-y^2}$ symmetry with nodes crossing the Fermi surface. Most important is the observation of the linear temperature dependence of the London penetration depth at low temperatures [2] which was discussed earlier by Annett *et al.* [3]. Such a linear dependence at low temperatures has also

been reported for the spin susceptibility [4]. More evidence was supplied by the discovery of the existence of the so-called unitary limit in the electronic thermal conductivity of YBCO single crystals doped with Zn [5], and the c -axis Josephson tunnelling experiments where the conventional superconductor (Pb) is deposited across a single twin boundary [6]. This experiment also offers a direct evidence for a subdominant s -symmetric contribution to the order parameter which is typical of orthorhombic systems [7].

Modifications in the low-temperature linear dependence of the penetration depth brought about by the impurity scattering [8] are also naturally understood from theoretical models with the order parameter having d -wave symmetry [9,10]. Such models, however, tend to predict slopes for the penetration depth near the critical temperature which are not as steep as those observed. This is true even if inelastic scattering is incorporated in the calculations through the Eliashberg-type formalism which represents a first approximate attempt of including self-energy effects [11].

Another set of experiments which can be used to put constraints on possible mechanisms of high T_c superconductivity are microwave conductivity measurements as a function of temperature in pure single crystals of optimally doped YBCO [12,13] which have revealed the existence of a very large peak around 40 K, whose size and position depend somewhat on the microwave frequency used. A similar peak can be found in the electronic thermal conductivity, though at much lower temperatures [14]. This peak in the microwave conductivity has been widely interpreted to be due to the rapid reduction in the inelastic scattering below T_c and is generally referred to as the collapse of the low-temperature inelastic scattering rate. One possible way to describe this experimental result is the introduction of a temperature dependent inelastic scattering time which can be modelled from the spin fluctuation theory [15].

Schachinger *et al.* [16–18] proposed quite a different explanation which not only allowed a satisfying analysis of the microwave conductivity peak but also described the temperature dependence of the London penetration depth and of the electronic thermal conductivity consistently. Their phenomenological model is based first of all on the observation that a mechanism responsible for superconductivity in oxides, which also leads to d -wave superconductivity, is most likely to be electronic in origin. In such a model the collapse of the inelastic scattering rate which causes a large peak in the microwave conductivity is explained by a gap which opens up in the fluctuation spectrum responsible for superconductivity [19–21]. Such an effect is generic to all electronic mechanisms where the fluctuation spectrum causing superconductivity belongs to the superconducting quasiparticle system itself and becomes gapped as superconductivity sets in.

The phenomenological model consists in the application of a temperature dependent low frequency cutoff to the fluctuation spectrum to give the correct temperature dependence of the London penetration depth of clean, optimally doped YBCO single crystals. (It is interesting to note that the temperature dependence of the low frequency cutoff follows quite closely the temperature dependence of

the superconducting gap.) This model is then used (within the framework of the Eliashberg-type formalism adjusted to allow for d -wave superconductivity) to calculate optical conductivity, microwave conductivity, and electronic thermal conductivity of clean superconductors and superconducting systems which also contain moderate concentrations of impurities.

It is the purpose of this paper to review the recent results and to expand the application of the model to the calculation of the optical conductivity of a $d_{x^2-y^2}$ superconductor in its normal as well as superconducting state. Section 2 specifies the basic Eliashberg-like equations and the formulae used to calculate the London penetration depth, optical conductivity, optical reflectivity, and electronic thermal conductivity. In Section 3 the results are discussed and, finally, Section 4 presents our conclusions.

2. Formalism

The simplest description of a d -wave superconductor is obtained within the BCS formalism assuming a separable model for the pairing interaction. In such a model the pairing potential depends on the product $\cos(2\theta)\cos(2\theta')$ where θ and θ' are the directions of the initial and final momenta on a two-dimensional circular Fermi surface. To include the dynamics of the fluctuations that are exchanged in the pairing it is necessary to go beyond the BCS and consider self-energy corrections. We restrict ourselves to the Eliashberg-type formalism which was discussed by Schachinger and Carbotte [22] and offers at least a first order approximation to the full self-energy corrections. Such a formalism includes a Bose-exchange spectral density $I^2F(\Omega)$ which enters both the gap channel for the pairing energy $\tilde{\Delta}(i\omega_n)$ and the channel for the renormalized Matsubara frequencies $\tilde{\omega}(i\omega_n)$. This last quantity exists in the normal state and carries information on the s -wave part of the interaction. From symmetry considerations, the gap channel involves the d -wave part of the interaction. In principle, these two projections of the full boson-exchange interaction need not involve the same weighting of the Bose energies. In the absence of detailed information on the mechanism we will assume, for simplicity, that a single $I^2F(\Omega)$ can, nevertheless, be employed as a first approximation but with a different weight g in the gap channel as compared to the renormalization channel. The two nonlinear self-energy equations for $\tilde{\omega}(i\omega_n)$ and $\tilde{\Delta}(i\omega_n)$, with $i\omega_n = i\pi T(2n+1)$, $n = 0, \pm 1, \pm 2, \dots$, and temperature T will then have the following form in the imaginary axis notation [22]:

$$\tilde{\omega}(i\omega_n) = \omega_n + \pi T \sum_m \lambda(m-n)\Omega(i\omega_m) + \pi\Gamma^+ \frac{\Omega(i\omega_n)}{c^2 + \Omega^2(i\omega_n) + D^2(i\omega_n)} \quad (1)$$

$$\tilde{\Delta}(i\omega_n, \theta) = g\pi T \sum_m \sqrt{2} \cos(2\theta)\lambda(m-n)D(i\omega_m) \quad (2)$$

$$\text{with} \quad \Omega(i\omega_n) = \left\langle \frac{\tilde{\omega}(i\omega_n)}{\sqrt{\tilde{\omega}^2(i\omega_n) + \tilde{\Delta}^2(i\omega_n, \theta)}} \right\rangle_{\theta} \quad (3)$$

$$D(i\omega_n) = \left\langle \frac{\sqrt{2} \cos(2\theta) \tilde{\Delta}(i\omega_n, \theta)}{\sqrt{\tilde{\omega}^2(i\omega_n) + \tilde{\Delta}^2(i\omega_n, \theta)}} \right\rangle_{\theta}, \quad (4)$$

and

$$\lambda(m-n) = 2 \int_0^{\infty} d\Omega \frac{\Omega I^2 F(\Omega)}{\Omega^2 + (\omega_m + \omega_n)^2}. \quad (5)$$

Here $\langle \dots \rangle_{\theta}$ denotes the average over the angle θ , $\Gamma^+ = n_I / (N(0)\pi^2)$ with n_I being the concentration of isotropically scattering impurities, $N(0)$ is the normal state quasiparticle density of states at the Fermi energy, $c = \cot \delta_0$, and δ_0 is the T-matrix phase shift. For very large values of c ($c \rightarrow \infty$) we are in the Born scattering limit and for $c = 0$ in the so-called unitary (resonant) scattering limit. In the weak scattering (Born) limit the impurity term in equation (1) reduces to $\pi t^+ \Omega(i\omega_n)$ with c absorbed into $t^+ = n_I N(0) |V(k_F)|^2$, where $V(k_F)$ is the impurity scattering potential evaluated at the Fermi momentum k_F .

The London penetration depth $\lambda_L(T)$ at any temperature $T < T_c$ follows from the solution of equations (1) and (2) and is given, within a numerical constant, by [10]:

$$\frac{1}{\lambda_L^2(T)} \propto \pi T \left\langle \sum_m \frac{\tilde{\Delta}^2(i\omega, \theta)}{[\tilde{\omega}^2(i\omega_n) + \tilde{\Delta}^2(i\omega_n, \theta)]^{3/2}} \right\rangle_{\theta}. \quad (6)$$

The optical conductivity $\sigma(\nu)$ at any temperature T and photon frequency ν is given by [23,24]:

$$\begin{aligned} \sigma(\nu) = & \frac{i e^2 N(0) v_F^2}{\nu} \frac{2}{2} \\ & \times \left\langle \int_0^{\infty} d\Omega \tanh\left(\frac{\Omega}{2T}\right) \frac{1 - N(\Omega, \theta)N(\Omega + \nu, \theta) - P(\Omega, \theta)P(\Omega + \nu, \theta)}{E(\Omega, \theta) + E(\Omega + \nu, \theta)} \right. \\ & + \int_0^{\infty} d\Omega \tanh\left(\frac{\Omega + \nu}{2T}\right) \frac{1 - N(\Omega, \theta)^*N(\Omega + \nu, \theta)^* - P(\Omega, \theta)^*P(\Omega + \nu, \theta)^*}{E(\Omega, \theta)^* + E(\Omega + \nu, \theta)^*} \\ & + \int_0^{\infty} d\Omega \left[\tanh\left(\frac{\Omega + \nu}{2T}\right) - \tanh\left(\frac{\Omega}{2T}\right) \right] \\ & \times \frac{1 + N(\Omega, \theta)^*N(\Omega + \nu, \theta) + P(\Omega, \theta)^*P(\Omega + \nu, \theta)}{E(\Omega + \nu, \theta) - E(\Omega, \theta)^*} \\ & + \int_{-\nu}^0 d\Omega \tanh\left(\frac{\Omega + \nu}{2T}\right) \left\{ \frac{1 - N(\Omega, \theta)^*N(\Omega + \nu, \theta)^* - P(\Omega, \theta)^*P(\Omega + \nu, \theta)^*}{E(\Omega, \theta)^* + E(\Omega + \nu, \theta)^*} \right. \\ & \left. + \frac{1 + N(\Omega, \theta)^*N(\Omega + \nu, \theta) + P(\Omega, \theta)^*P(\Omega + \nu, \theta)}{E(\Omega + \nu, \theta) - E(\Omega, \theta)^*} \right\} \Bigg\rangle_{\theta}, \quad (7) \end{aligned}$$

where the star symbolizes a complex conjugate, e is a charge on the electron, and v_F is the Fermi velocity. Furthermore,

$$E(\nu, \theta) = \sqrt{\tilde{\omega}^2(\nu) - \tilde{\Delta}^2(\nu, \theta)}, \quad (8)$$

$$N(\nu, \theta) = \frac{\tilde{\omega}(\nu)}{E(\nu, \theta)}, \quad (9)$$

$$P(\nu, \theta) = \frac{\tilde{\Delta}(\nu, \theta)}{E(\nu, \theta)}. \quad (10)$$

In the normal state equation (7) can be replaced by [23]:

$$\begin{aligned} \sigma(\nu) = & \frac{\omega_p^2}{4\pi} \frac{1}{i\nu} \left\{ \int_{-\infty}^0 d\Omega \tanh\left(\frac{\nu + \Omega}{2T}\right) S^{-1}(T, \nu, \Omega) \right. \\ & \left. + \int_0^{\infty} d\Omega \left[\tanh\left(\frac{\nu + \Omega}{2T}\right) - \tanh\left(\frac{\Omega}{2T}\right) \right] S^{-1}(T, \nu, \Omega) \right\}, \quad (11) \end{aligned}$$

with ω_p – the plasma frequency,

$$S(T, \nu, \Omega) = \nu + \Sigma(T, \nu + \Omega)^* - \Sigma(T, \Omega) - i\pi t^+, \quad (12)$$

and

$$\Sigma(T, \omega) = - \int dz I^2 F(z) \left[\psi\left(\frac{1}{2} + i\frac{\omega + z}{2\pi T}\right) - \psi\left(\frac{1}{2} + i\frac{\omega - z}{2\pi T}\right) \right]. \quad (13)$$

Here $\psi(z)$ is a digamma function of complex argument z .

Once the real ($\sigma_1(\nu)$) and imaginary ($\sigma_2(\nu)$) parts of the conductivity are known, the optical reflectivity $R(\nu)$ can easily be calculated using

$$R(\nu) = \left| \frac{1 - \sqrt{\varepsilon(\nu)}}{1 + \sqrt{\varepsilon(\nu)}} \right|^2, \quad (14)$$

with the dielectric function $\varepsilon(\nu)$ defined as

$$\varepsilon(\nu) = \varepsilon_0 + \frac{4\pi}{\nu} i\sigma(\nu), \quad (15)$$

where ε_0 describes the response of quasiparticles in completely filled bands.

Using the above notation we find for the electronic thermal conductivity [25]:

$$\begin{aligned} \kappa_{ab,e}(T) = & \frac{2N(0)v_F^2}{T^2} \int_0^{\infty} \frac{d\nu \nu^2}{\cosh^2(\nu/2T)} \\ & \times \left\langle \frac{1 + N_1^2(\nu; \theta) + N_2^2(\nu; \theta) - P_1^2(\nu; \theta) - P_2^2(\nu; \theta)}{E_2(\nu; \theta)} \right\rangle_{\theta}. \quad (16) \end{aligned}$$

where indices 1 and 2 refer to the real and imaginary parts, respectively. equations (7) to (16) require the renormalized gap function $\tilde{\Delta}(\nu)$ and the renormalized frequencies $\tilde{\omega}(\nu)$ on the real axis. These can be found by the analytical continuation of the results of equations (1) and (2) from the imaginary axis to the real one employing the method developed by Marsiglio *et al.* [26].

Most of the parameters of the model have now been specified except for g , the d - to s -anisotropy of the exchange potential and for the form of the boson-exchange spectral density $I^2F(\Omega)$ which describes the fluctuation spectrum. Many choices could be made for this latter quantity. If we knew the actual mechanism which leads to pairing in oxides, there would be no choice at all as we would know the microscopic origin. In the absence of such information we adopt a very simple form which can be regarded as one guided by the nearly antiferromagnetic Fermi liquid model [27,28]. We use

$$I^2F(\Omega) = I^2 \frac{\Omega/\omega_{sf}}{1 + (\Omega/\omega_{sf})^2} \quad (17)$$

up to to some convenient high frequency cutoff for the numerical work (400 meV here). The frequency ω_{sf} sets the energy scale of the fluctuation spectrum and is not arbitrary because our numerical work has to reflect the observation that above the critical temperature the inelastic scattering rate is of the order of several times T_c in value. This requires $\omega_{sf} = 30$ meV and I^2 is adjusted to give a clean limit critical temperature $T_{c0} = 100$ K in solving the linearized equations (1) and (2) [16]. This results in the strong coupling parameter $T_{c0}/\omega_{log} = 0.31$ where ω_{log} is defined in the usual way [29]

$$\omega_{log} = \exp \left\{ \frac{2}{\lambda} \int d\Omega \frac{I^2F(\Omega)}{\Omega} \ln \Omega \right\}, \quad (18)$$

and represents the average boson energy in the system. The only parameter left is g and it has already been shown that the results do not depend qualitatively on the choice of g [16] and we set $g = 0.8$ to be definite.

3. Results

3.1. Optical conductivity, normal state

It is the aim of this short subsection to verify the parameters introduced previously to make the fluctuation spectrum (17) definite, namely, ω_{sf} , and the high frequency cutoff, by comparing the theoretically obtained normal state conductivity, equation (11), with the experiment. Figure 1 presents the results of such a comparison. What is shown here is the real part of the optical conductivity $\sigma_1(\nu)$ (figure 1a) and the inverse of the in-plane optical scattering time

$$\frac{1}{\tau_{ab}(\nu)} = \frac{\omega_p}{4\pi} \Re \left[\frac{1}{\sigma(\nu)} \right] \quad (19)$$

as a function of frequency ν . The data points are for a clean, twinned, optimally

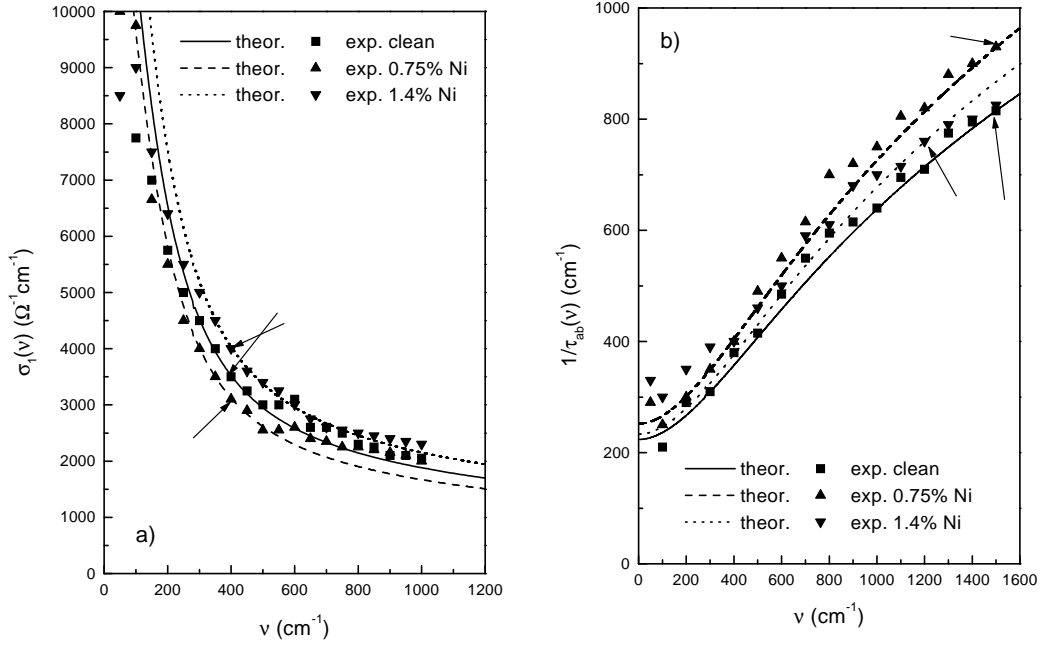


Figure 1. a) The real part of the normal state optical conductivity $\sigma_1(\nu)$ and b) the inverse optical scattering time $1/\tau_{ab}(\nu)$ as a function of frequency ν . The data points represent experimental data reported by Homes *et al.* [30] for a clean, twinned, optimally doped YBCO single crystal (solid squares), for a similar sample with 0.75% Ni substitution (solid triangles), and for a sample with 1.4% Ni (solid down-triangles). Theoretical results obtained from equation (11) are shown for the clean sample (solid line), the sample with 0.75% Ni (dashed line), and for the sample with 1.4% Ni (dotted line). The arrows indicate the data points used to scale theory to experiment. The temperature is 100 K.

doped YBCO single crystal ($T_c = 93.2\text{ K}$, solid squares), a similar sample with 0.75% Ni substituted at Cu-sites ($T_c = 91\text{ K}$, solid triangles), and a sample with 1.4% Ni substitution ($T_c = 89\text{ K}$, solid down-triangles). The normal state conductivity data have been obtained at a sample temperature of 100 K in all the cases. Theoretical results are presented for the clean sample (solid line), the sample with 0.75% Ni (dashed line), and the sample with 1.4% Ni (dotted line). The Ni content was simulated by the value for t^+ necessary to decrease the clean sample's critical temperature to the required value. The arrows indicate the data points used to scale theory to experiment. This scaling was necessary as the theoretical results are on an arbitrary scale because of the factor $\omega_p/4\pi$ which was left out in evaluating equation (11). Theoretically such a scaling should not be necessary for the inverse scattering time because, according to equation (19), the theoretical values are free of this material parameter. Nevertheless, Homes *et al.* [30] point

out in their paper that they were using a value of $\omega_p = 1.6 \text{ eV}$ which is somewhat ambiguous because it depends on the frequency cutoff used in the evaluation of the experimental data.

The agreement between theory and experiment is excellent for the clean and the 0.7% Ni sample over the whole frequency range covered by the experiment. We note some deviations for the 1.4% Ni sample at low frequencies and above 1200 wave numbers. But it is quite obvious that this data set escapes the general trend established by the other two samples.

We conclude that the simple model fluctuation spectrum (17) with $\omega_{sf} = 30 \text{ meV}$ and a high frequency cutoff of 400 meV allow an excellent description of the frequency dependence of the normal state optical conductivity and thus, establishes a valid basis for further investigations into the superconducting state.

3.2. In-plane London penetration depth

Our results for the temperature dependence of the in-plane London penetration depth given on evaluation of equation (6) which requires only the solutions of the self-energy equations (1) and (2) on the imaginary axis are displayed in figure 2. What is presented is the inverse square of the normalized in-plane penetration

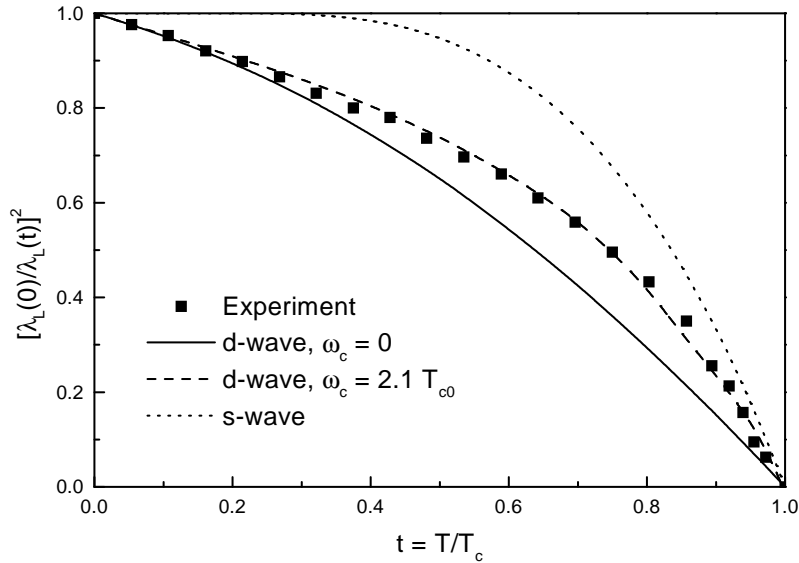


Figure 2. The inverse square of the normalized in-plane London penetration depth $[\lambda_L(0)/\lambda_L(t)]^2$ as a function of the reduced temperature $t = T/T_c$. The solid curve is for a $d_{x^2-y^2}$ superconductor and without a low frequency cutoff in the fluctuation spectrum. The dashed curve is for a low frequency cutoff $\omega_c = 2.1T_c$ in the fluctuation spectrum. The solid squares indicate the data by Bonn *et al.* [31]. Finally, the dotted line gives the results one would get for a classical s -wave superconductor like Pb.

depth $[\lambda_L(0)/\lambda_L(t)]^2$ as a function of the reduced temperature $t = T/T_c$. The experimental data by Bonn *et al.* [31] are indicated by solid squares. It is obvious from the figure that these data cannot be described by an s -wave superconductor (dotted line). On the other hand, the low temperature results for a $d_{x^2-y^2}$ superconductor (solid line) seem to agree rather well with the experiment in the region $0 \leq t \leq 0.2$ but for $t > 0.2$ very pronounced deviations are noted. In particular, as in the previous work [11], the slope of the penetration depth near T_c is not so steep as compared with the experiment.

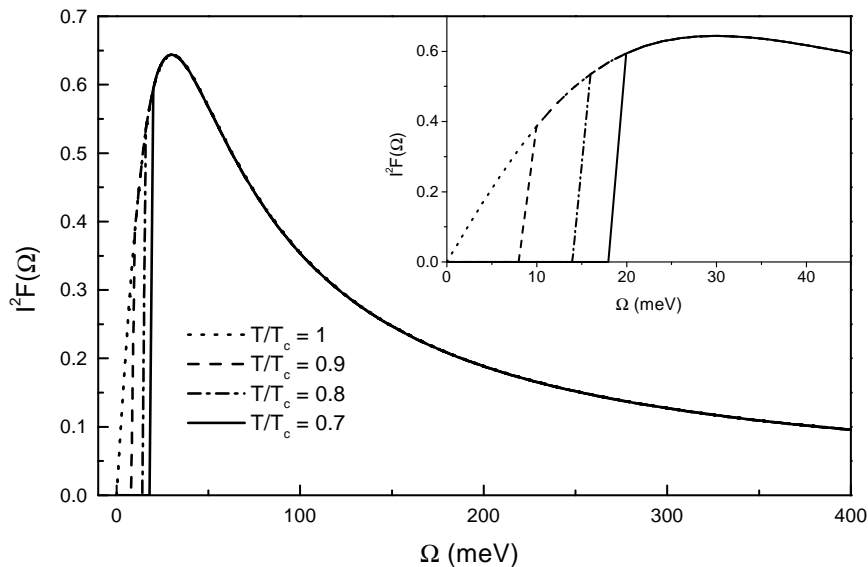


Figure 3. The fluctuation spectrum $I^2F(\Omega)$ according to equation (17). We present spectra for four different temperatures, namely, $T/T_c = 1$ (dotted line), $T/T_c = 0.9$ (dashed line), $T/T_c = 0.8$ (dash-dotted line), and $T/T_c = 0.7$ (solid line). At $T/T_c = 0.7$ the full low frequency cutoff $\omega_c = 2.1T_c$ is in effect. The insert shows the low frequency part of the fluctuation spectrum on an extended frequency scale.

In order to develop a theoretical model able to remove this discrepancy between theoretical predictions and the experiment we recall the result well known from functional derivative methods and applied to conventional anisotropic s -wave superconductors, namely, that very low frequency phonons have the same effect as static impurities and reduce T_c , i.e., they are pair breaking [32]. Similar considerations apply to a d -wave superconductor in which case it has been shown that the functional derivative of T_c with the fluctuation spectral density is negative at low frequencies [33]. If, at low temperatures, such low-energy excitations are removed because of the feedback effect superconductivity has on the fluctuation spectrum, one would expect that the superconducting gap itself will be larger than it would otherwise be for the associated value of T_c . With the increase of

temperature the amount of pair breaking increases, because the low frequency part of the fluctuation spectrum is restored as the superconducting gap closes up. This should affect the temperature dependence of the penetration depth. In fact, the experimental data of Bonn *et al.* [31] can be used to model the temperature dependence of such a low frequency cutoff to make the theoretical results follow quantitatively the experiment. If we apply a low frequency cutoff $\omega_c = 2.1T_{c0}$ at $t = 0$ to the fluctuation spectrum and model the temperature dependence of ω_c closely to that of the superconducting gap, we achieve, after minor adjustments, optimal agreement between theory and experiment (dashed line, figure 2). This fluctuation spectrum, which will also be used in all further calculations, is presented in figure 3 where the temperature dependence of the low frequency cutoff is emphasized in the insert which shows the low frequency part of the fluctuation spectrum on an extended frequency scale for various reduced temperatures. Obviously, what pushes up $[\lambda_L(0)/\lambda_L(t)]^2$ at intermediate temperatures and, correspondingly, increases the slope near T_c , is the pair breaking effect associated with the introduction of lower frequency fluctuations as T increases towards T_c .

3.3. Microwave conductivity

In discussing the microwave conductivity we concentrate on the case $\nu = 34.8 \text{ GHz} \simeq 0.144 \text{ meV}$ studied by Bonn *et al.* [12] using a clean, twinned, and optimally doped YBCO single crystal. It has already been pointed out by Schachinger *et al.* [16,17] that the peak in the microwave conductivity of a $d_{x^2-y^2}$ superconductor falls too low in temperature and is not large enough to agree with the experiment if equations (1) and (2) are solved in a clean limit employing an unmodified fluctuation spectrum (17) before equation (15) is solved to calculate optical conductivity. But applying a low frequency cutoff to (17) according to figure 3 moves the microwave peak towards higher temperatures and increases its magnitude considerably bringing the theoretical predictions into better but still not satisfying agreement with the experiment.

Adding impurity scattering in the Born approximation affects the size and width of the microwave peak with the position of the peak in temperature remaining relatively unchanged. If, instead, the impurity scattering is treated in the unitary limit, the attenuation of the microwave peak is much more pronounced and shifts to higher temperatures [17]. While in the best untwinned single crystal samples of YBCO the residual scattering is believed to be rather small, we have to assume for twinned crystals some residual scattering which can be modelled by adding some Born limit impurity scattering to achieve the best possible agreement between theory and experiment. Figure 4 shows the result of such a fitting process in which the impurity parameter $t^+ = 0.822 \text{ meV}$ has been chosen which reduces the clean limit critical temperature by 5 K to $T_c = 95 \text{ K}$. (The solid squares in figure 4 correspond to the experimental data reported by Bonn *et al.* [12] and the solid curve gives our best theoretical result.) The scale in our theoretical data is arbitrary and was fitted to agree with the data at the temperature indicated by the arrow. For comparison we also show in figure 4 the theoretical result one

would get if the system's critical temperature were lowered to 95 K by adding the resonant impurity scattering (the dotted line). While for the Born scattering excellent agreement is obtained, the unitary impurity scattering results certainly provide an unacceptable description of the data.

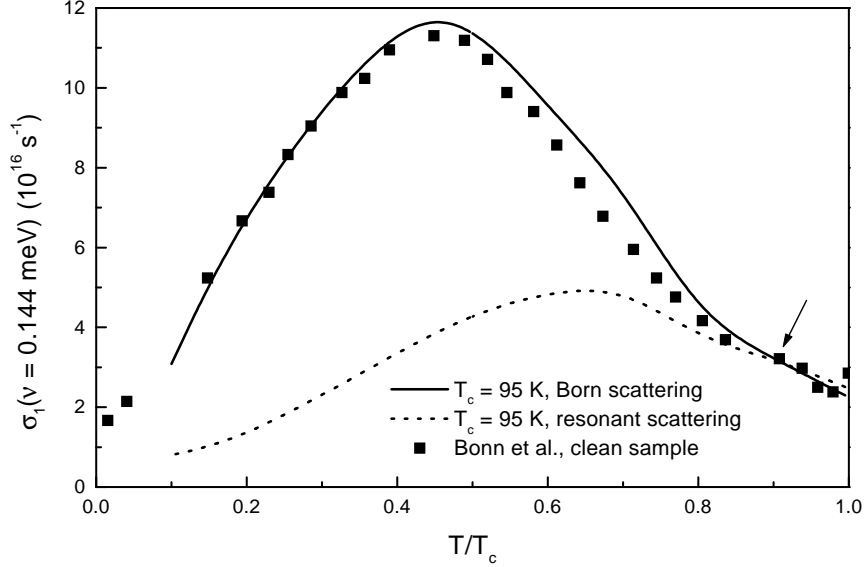


Figure 4. The real part of the microwave conductivity, σ_1 , for the frequency $\nu = 34.6 \text{ GHz} \simeq 0.144 \text{ meV}$ as a function of the reduced temperature T/T_c . The solid line represents the theoretical results for a model system having T_c of 95 K as a result of the additional Born impurity scattering. The dotted line corresponds to a model system with the additional resonant impurity scattering having the same T_c as the former system. In both systems a low frequency cutoff of $\omega_c = 2.1T_c$ at zero temperature has been applied to the fluctuation spectrum $I^2F(\Omega)$. The solid squares correspond to experimental data reported by Bonn *et al.* [8] for a clean, twinned, optimally doped YBCO single crystal. The arrow indicates the data point which has been used to scale theory to experiment.

This establishes the theoretical equivalent of a clean and twinned YBCO single crystal and completely defines the phenomenological model by the temperature dependence of the low-frequency cutoff in the fluctuation spectrum responsible for superconductivity and by a certain amount of the Born impurity scattering to compensate for the residual scattering in a clean, twinned sample. If this model is to be used to define additional constraints on possible theoretical explanations of high T_c superconductivity, predictions of this model are to be compared with other properties of clean and twinned YBCO single crystals which do not need additional theoretical parameters and do not depend linearly on the properties investigated so far.

3.4. Electronic thermal conductivity

A candidate, for which experimental data are readily available, is the electronic thermal conductivity. While the normal state electronic thermal conductivity is linearly related to the d.c. conductivity ($\nu = 0$) via the Wiedemann-Franz law, there is certainly no linear relation between the microwave conductivity ($\nu \neq 0$) and the electronic thermal conductivity, as a close inspection of equations (7) or (15) and (16) reveals immediately. It has already been pointed out in the introduction that the in-plane electronic thermal conductivity, $\kappa_{ab,e}(T)$, of clean, twinned YBCO single crystals develops a very pronounced low temperature peak in its temperature dependence. This feature can now be used to check on the consistency of the model developed so far.

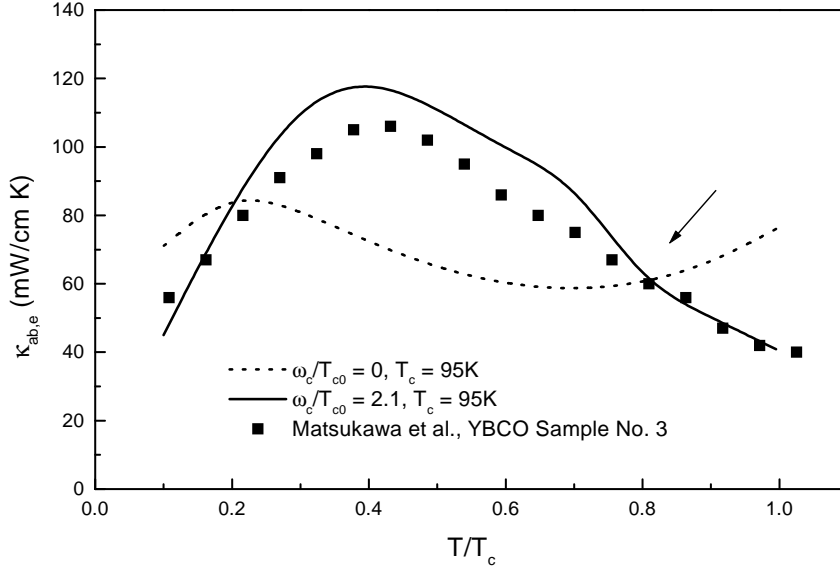


Figure 5. The in-plane electronic thermal conductivity $\kappa_{ab,e}(T)$ in units of mW/cm K as a function of the reduced temperature T/T_c . The solid curve is the result of model calculations using a temperature dependent low frequency cutoff in the fluctuation spectrum. The solid squares are the data of Matsukawa *et al.* [14] and seem to agree well with theory. The scale of the theoretical $\kappa_{ab,e}(T)$ was adjusted to fit the point indicated by the arrow. The dotted line is a theoretical calculation without a low frequency cutoff on the fluctuation spectrum. It disagrees strongly with the data.

Schachinger and Carbotte [18] demonstrated in an extensive study that $\kappa_{ab,e}(T)$ does not show in the clean limit of equations (1) and (2) a very pronounced peak around $t = 0.15$ if the unmodified fluctuation spectrum (17) is applied. This peak is then enhanced by at least one order of magnitude if the temperature dependent low frequency cutoff of the fluctuation spectrum is included. No significant shift

of the peak in temperature occurs. Adding impurities attenuates the peak and it becomes shifted towards higher temperatures. In this, again, the Born impurity scattering is less effective than resonant scattering impurities.

Without the introduction of any new parameters, the theoretical results of calculations within the phenomenological model are scaled to meet the in-plane electronic thermal conductivity measured by Matsukawa *et al.* [14], as shown in figure 5 (the solid line). (This scaling is still necessary because in order to set the scale theoretically the value $N(0)v_F^2$ of equation (16) is needed but it is not known. Thus, a fit to one data point, indicated by the arrow in figure 5, is essential.) Without the low frequency cutoff the dashed curve is obtained which shows no agreement with the experiment at all. Thus, the in-plane electronic thermal conductivity is an equally sensitive probe of the feedback effect which superconductivity has on the fluctuation spectrum.

3.5. Microwave conductivity in systems with impurities

After the phenomenological model has been defined and verified against the in-plane electronic thermal conductivity, it is certainly of some interest to test it even further using experimental results reported by Bonn *et al.* [8] for the microwave conductivity of twinned YBCO single crystals which have been doped with small concentrations of Zn and Ni. In particular, one sample with 0.3% Zn substitution at the Cu-sites showed a critical temperature of 89.5 K (about 4 K down from the clean sample's T_c) and the other sample with 0.71% Ni substitution had T_c of 90.47 K (about 3 K down). This alone establishes Zn as a more powerful dopant. The experiments also revealed that both types of impurities had about the same effect on the peak in the microwave conductivity (a substantial reduction to less than half the height of the clean sample and only a little shift towards higher temperatures). On the other hand, the in-plane penetration depth followed a T^2 law in its low temperature dependence in the Zn doped sample (typical of the resonant impurity scattering) while the Ni doped sample developed a linear low temperature dependence which is typical of the Born scattering [3,10]. This is the reason why Ni impurities have been regarded to be of the Born type.

The experimental situation can be simulated theoretically by either increasing t^+ beyond its clean sample value of 0.822 meV until the observed decrease in T_c by about 3.5 K on the average is achieved or by adding nonzero values of Γ^+ to describe additional resonant scattering impurities. It was pointed out by Schachinger and Carbotte [17] that only resonant scattering impurities have the observed effect on the peak of the microwave conductivity. As Ni does not show the required T^2 law in the low temperature variation of the in-plane penetration depth, these authors concluded that Ni impurities must be at least of intermediate scattering strength and setting $c = 0.5$ in equation (1) results in excellent agreement between the experimental and theoretical microwave conductivity data even for Ni doped YBCO. This is demonstrated in figure 6a. Schachinger and Carbotte [17] were also able to prove that the T^2 to T law crossover in the low temperature variation of the in-plane penetration depth occurs in the region $0.3 < c < 0.4$ and this explains

why the theoretical predictions for the low temperature variation of the in-plane penetration depth agree so well with the experiment, as it is shown in figure 6b.

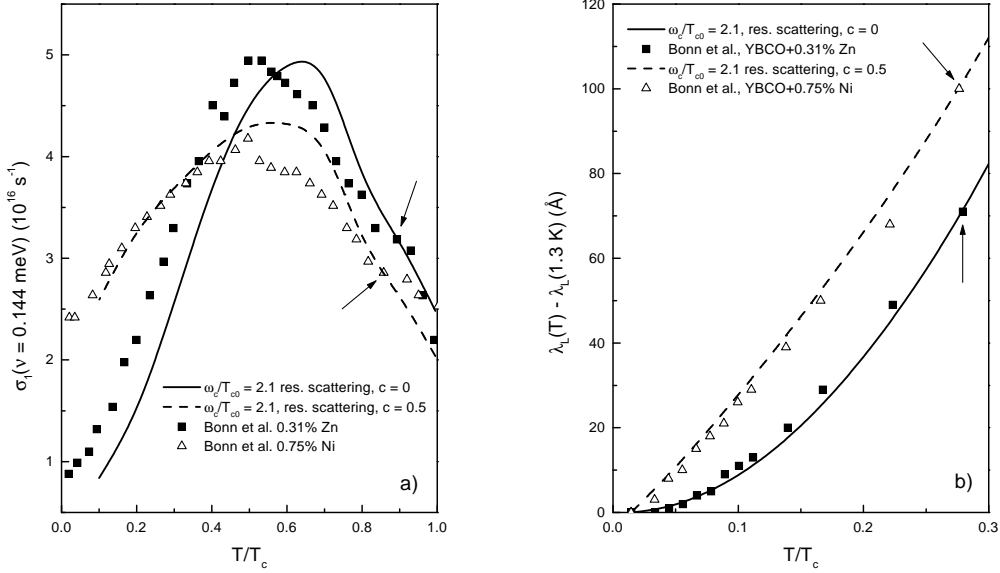


Figure 6. a) The real part of the microwave conductivity, σ_1 , for the frequency of $\nu = 34.8 \text{ GHz} = 0.144 \text{ meV}$; b) the difference in the London penetration depth $\lambda_L(T) - \lambda_L(1.3 \text{ K})$ as a function of the reduced temperature T/T_c . The solid line represents the theoretical results for a model system the critical temperature of which has been lowered from 95 K to 91.5 K by the resonant impurity scattering ($c = 0$). The dashed line corresponds to a model system of the same $T_c = 91.5 \text{ K}$ but with the intermediate strength impurity scattering ($c = 0.5$). In both systems a low frequency cutoff $\omega_c = 2.1T_{c0}$ at zero temperature had been applied to the fluctuation spectrum. The solid squares represent the experimental data for a YBCO sample with 0.31% Zn substitution, while the open triangles describe the experimental data for a YBCO sample with Ni substitution [8]. The arrows indicate the data points which have been used to scale theory to experiment.

All this proves that a phenomenological model which describes the feedback the superconductivity has on a fluctuation spectrum belonging to the same system of quasiparticles which condense is capable of a consistent description of the temperature dependence of various properties of optimally doped samples of YBCO with and without additional doping with Zn or Ni impurities. In the next subsection we would like to investigate how the frequency dependence of the optical conductivity is affected by the model assumptions and how this agrees with the experiment.

3.6. Optical conductivity, superconducting state

In figure 7a we compare the optical reflectivity $R(\nu)$ and the real part of the optical conductivity $\sigma_1(\nu)$ with the data reported by Wang *et al.* [34] for an untwinned, optimally doped, clean YBCO single crystal ($T = 8$ K) and with the data measured by Homes *et al.* [30] for a similar sample ($T = 12$ K). These authors also

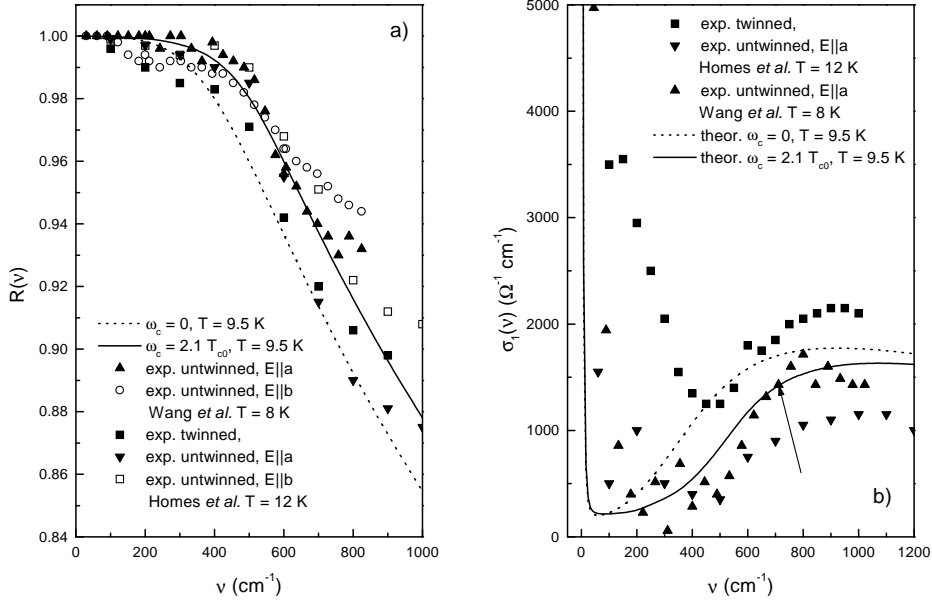


Figure 7. a) The reflectivity $R(\nu)$ and b) the real part of the optical conductivity $\sigma_1(\nu)$ as a function of frequency ν . Theoretical data are presented for the theoretical equivalent of a clean sample with (solid lines) and without (dotted lines) a low frequency cutoff in the fluctuation spectrum. The temperature is 9.5 K. Included are the experimental data reported by Wang *et al.* [34] for a clean, untwinned, optimally doped YBCO single crystal. The sample temperature is 8 K, the solid triangles correspond to the light polarized along the a axis ($E||a$) while the open circles are for $E||b$. The other data are from the experiments by Homes *et al.* [30] and are for a clean, untwinned, optimally doped YBCO single crystal and a sample temperature 12 K. The solid down-triangles correspond to $E||a$ and the open squares to $E||b$. Finally, data for a clean, twinned, optimally doped YBCO single crystal are also included (solid squares).

report data for a twinned, optimally doped, clean YBCO single crystal. Theoretical results are presented for the theoretical equivalent of the clean sample without (the dotted line) and with (the solid line) a low frequency cutoff $\omega_c = 2.1T_{c0}$ at zero temperature. We also used $\varepsilon_0 = 3.5$, $\omega_p = 1.6$ eV, and $T = 9.5$ K. Obviously, the theoretical data for a system with the low frequency cutoff in the fluctuation spectrum are in better agreement with the experiment. It is also interesting to

note that the best agreement can be found for the $E||a$ data of untwinned samples (the solid triangles and the solid down-triangles). This is not surprising as the light polarized along the a -axis probes just the CuO_2 planes and the theory presented here is developed to describe superconductivity in two-dimensional copper-oxygen planes. The worst agreement between theory and experiment is found for the twinned sample (the solid squares). This shows that our theoretical equivalent of the twinned clean sample is not sufficient to describe completely the influence the background scattering has on the optical conductivity at higher frequencies.

A similar comparison can be found in figure 7b for the real part of the optical conductivity $\sigma_1(\nu)$ as a function of frequency ν . The theoretical results for the system with the low frequency cutoff in the fluctuation spectrum have been scaled to fit the data point indicated by the arrow. Using a slightly different scaling would have provided an almost equally good agreement with the data reported by Homes *et al.* (the solid down-triangles). The same scaling was then applied to the system with the full fluctuation spectrum. The main feature of these results is that the low frequency cutoff in the fluctuation spectrum suppresses the real part of the optical conductivity to higher frequencies, thus indicating a bigger gap than one would find without such a low frequency cutoff. This is in very good agreement with the $E||a$ data for the untwinned sample in the region of $200 < \nu < 1000$ wave numbers which is quite remarkable. Again, no agreement at all is found for the twinned sample developing a frequency dependence of $\sigma_1(\nu)$ which would correspond to a much higher impurity content as it is required by the critical temperature.

4. Conclusion

Experimental evidence is very much in favour of a superconducting order parameter which is predominantly of a d -wave symmetry. In orthorhombic systems a subdominant component of a s -wave symmetry can be expected. A mechanism which is responsible for the superconductivity in oxides and which also results in a d -wave symmetry of the superconducting order parameter is most likely to be electronic in origin (no phonons).

In this paper a phenomenological model developed by Schachinger *et al.* [16–18] has been discussed and proved to be able to describe consistently the temperature dependence of the in-plane penetration depth, the temperature dependence of the microwave conductivity and of the electronic thermal conductivity of clean, twinned and optimally doped YBCO single crystals. Moreover, calculations performed within the framework of this model revealed that the influence of impurities of various kinds on the temperature dependence of the microwave conductivity and of the in-plane penetration depth can also be explained consistently. Finally, it was possible to demonstrate in this paper that the model is also capable to predict a frequency dependence of the low temperature optical conductivity which is in very good agreement with the experimental data found for the light polarized along the a -axis of untwinned, clean, optimally doped YBCO single crystals.

These results will now be used to put additional constraints on possible mecha-

nisms of superconductivity in oxides: it is not only most likely that the mechanism is electronic in origin leading to a d -wave superconductivity. Moreover, it seems necessary for the fluctuation spectrum which causes superconductivity to belong to the superconducting quasiparticle system because it becomes gapped as the superconductivity sets in. This has been demonstrated quite clearly by the phenomenological model discussed here.

Acknowledgements

The authors are greatly indebted to Prof. Dr. J.P.Carbotte for his intensive collaboration and support. They would also like to thank Dr. C.C.Homes and Prof. Dr. T.Timusk for the access to their data prior to publication. This research was supported in part by Fonds zur Förderung der wissenschaftlichen Forschung (FWF), Vienna, Austria under contract No. P11890-NAW.

References

1. Bednorz J.G., Müller A. Possible high T_c superconductivity in the Ba-La-Cu-O system. // Z. Phys. B, 1986, vol. 64, p. 189–193.
2. Hardy W.N., Bonn D.A., Morgan D.C., Liang R., Zhang K. Precision measurements of the temperature dependence of λ in $\text{YBa}_2\text{Cu}_3\text{O}_{6.95}$: strong evidence for nodes in the gap function. // Phys. Rev. Lett., 1993, vol. 70, p. 3999–4002.
3. Annett J.F., Goldenfeld N., Renn S.R. The Pairing State of $\text{YBa}_2\text{Cu}_3\text{O}_{7-x}$. In: Physical Properties of High Temperature Superconductors. Vol. 2. Ed.: Ginsberg D.M. World Scientific, Singapore 1990, p. 571–685.
4. Jánossy V., Fehér T., Oszlány G., Williams G.V.M. Linear low temperature spin susceptibility in the underdoped high T_c superconductor, $\text{Gd:YBa}_2\text{Cu}_4\text{O}_8$. // Phys. Rev. Lett., 1997, vol 79, p. 2726–2729.
5. Taillefer L., Lussier B., Gagnon R. Universal heat conduction in $\text{YBa}_2\text{Cu}_3\text{O}_{6.9}$. // Phys. Rev. Lett., 1997, vol. 79, p. 483–486.
6. Kouznetsov K.A., Sun A.G., Chen B., Katz A.S., Bahcall R., Clarke J., Dynes R.C., Gajewski D.A., Han S.H., Maple M.B., Giapintzakis J., Kim J.-T., Ginsberg D.M. c -Axis Josephson tunneling between $\text{YBa}_2\text{Cu}_3\text{O}_{7-\delta}$ and Pb: direct evidence for mixed order parameter symmetry in a high- T_c superconductor. // Phys. Rev. Lett., 1997, vol. 79, p. 3050–3053.
7. Schürer I., Schachinger E., Carbotte J.P. Optical conductivity in orthorhombic d -wave superconductors. // Phys. Rev. B (submitted).
8. Bonn D.A., Kamal S., Zhang K., Liang R., Baar D.J., Klein E., Hardy W.N. Comparison of the influence of Ni and Zn impurities on the electromagnetic properties of $\text{YBa}_2\text{Cu}_3\text{O}_{6.95}$. // Phys. Rev. B, 1994, vol. 50, p. 4051–4063.
9. Graf M.J., Yip S-K., Sauls J.A., Rainer D. Electronic thermal conductivity and the Wiedemann-Franz law for unconventional superconductors. // Phys. Rev. B, 1996, vol. 53, p. 15147–15161.
10. Prohammer M., Carbotte J.P. London penetration depth of d -wave superconductors. // Phys. Rev. B, 1991, vol. 43, p. 5370–5374.

11. Carbotte J.P., Jiang C. Strong-coupling effects in d -wave superconductors. // Phys. Rev. B, 1993, vol. 48, p. 4231–4234.
12. Bonn D.A., Dosanjh P., Liang R., Hardy W.H. The microwave surface impedance of $\text{YBa}_2\text{Cu}_3\text{O}_{7-\delta}$. // J. Phys. Chem. Solids, 1995, vol. 56, p. 1941–1943.
13. Srikanth H., Willemsen B.A., Jacobs T., Sridhar S., Erb A., Walker E., Flükiger R. Microwave response of $\text{YBa}_2\text{Cu}_3\text{O}_{6.95}$ crystals: evidence for a multicomponent order parameter. // Phys. Rev. B, 1997, vol. 55, p. R14733–R14736.
14. Matsukawa M., Mizukoshi T., Noto K. In-plane and out-of-plane thermal conductivity of a large single crystal of $\text{YBa}_2\text{Cu}_3\text{O}_{7-x}$. // Phys. Rev. B, 1996, vol. 53, p. R6034–R6037.
15. Hensen S., Müller G., Rieck C.T., Scharnberg K. In-plane surface impedance of epitaxial $\text{YBa}_2\text{Cu}_3\text{O}_{7-\delta}$ films: comparison of experimental data taken at 87 GHz with d -wave and s -wave models of superconductivity. // Phys. Rev. B, 1997, vol. 56, p. 6237–6264.
16. Schachinger E., Carbotte J.P., Marsiglio F. Effect of suppression of the inelastic scattering rate on the penetration depth and conductivity in a $d_{x^2-y^2}$ superconductor. // Phys. Rev. B, 1997, vol. 56, p. 2738–2750.
17. Schachinger E., Carbotte J.P. Effect of impurity scattering on microwave conductivity of a $d_{x^2-y^2}$ superconductor. // Phys. Rev. B, 1998, (in print).
18. Schachinger E., Carbotte J.P. Inelastic scattering rate on thermal conductivity of a $d_{x^2-y^2}$ superconductor. // Phys. Rev. B, 1998, (in print).
19. Bourges P., Regnault L.P., Sidis Y., Vettier C. Inelastic neutron-scattering study of antiferromagnetic fluctuations in $\text{YBa}_2\text{Cu}_3\text{O}_{6.97}$ // Phys. Rev. B, 1996, vol. 53, p. 876–885.
20. Fong H.F., Keimer B., Anderson P.W., Reznik D., Dogan F., Aksay I.A. Phonons and magnetic scattering at 41 meV in $\text{YBa}_2\text{Cu}_3\text{O}_7$. // Phys. Rev. Lett., 1995, vol. 75, p. 316–319.
21. Bourges P., Sidis Y., Regnault L.P., Hennion B., Villeneuve B., Collin G., Vettier C., Henry J.Y., Marucco J.F. Comparison of antiferromagnetic fluctuations in zinc-free and zinc-doped YBCO in fully oxidized samples. Studies by inelastic neutron scattering. // J. Phys. Chem. Solids, 1995, vol. 56, p. 1937–1938.
22. Schachinger E., Carbotte J.P. Thermodynamics for retarded d -wave interaction and arbitrary impurity concentrations. // Phys. Rev. B, 1991, vol. 43, p. 10279–10288.
23. Lee W., Rainer D., Zimmermann W. Holstein effect in the far-infrared conductivity of high- T_c superconductors. // Physica C, 1989, vol. 159, p. 535–544.
24. Carbotte J.P., Jiang C., Basov C.N., Timusk T. Evidence for d -wave superconductivity in $\text{YBa}_2\text{Cu}_3\text{O}_{7-\delta}$ from far-infrared conductivity. // Phys. Rev. B, 1995, vol. 51, p. 11798–11805.
25. Ambegaokar V. Theory of the electronic thermal conductivity of superconductors with strong electron-phonon coupling. // Phys. Rev., 1964, vol. 134, p. A803–A815.
26. Marsiglio F., Schossmann M., Carbotte J.P. Iterative analytic continuation of the electron self-energy to the real axis. // Phys. Rev. B, 1988, vol. 37, p. 4965–4969.
27. Millis A.J., Monien H., Pines D. Phenomenological model of nuclear relaxation in the normal state of $\text{YBa}_2\text{Cu}_3\text{O}_7$. // Phys. Rev. B, 1990, vol. 37, p. 167–178.
28. Monthoux P., Balatsky A.V., Pines D. Weak-coupling theory of high-temperature superconductivity in the antiferromagnetically correlated copper oxides. // Phys. Rev. B, 1992, vol. 46, p. 14803–14817.
29. Carbotte J.P. Properties of boson-exchange superconductors. // Rev. Mod. Phys.,

- 1990, vol. 62, p. 1027–1157.
30. Homes C.C., Bonn D.A., Liang R.L., Hardy W.N., Basov D.N., Timusk T., Clayman B.P. The effect of Ni impurities on the optical properties of $\text{YBa}_2\text{Cu}_3\text{O}_{6+y}$: possible coupling between the a - b planes and the c axis dynamics. // In preparation.
 31. Bonn D.A., Dosanjh P., Liang R., Hardy W.H. Evidence for rapid suppression of quasi-particle scattering below T_c in $\text{YBa}_2\text{Cu}_3\text{O}_{7-\delta}$. // Phys. Rev. Lett., 1992, vol. 68, p. 2390–2393.
 32. Daams J.M., Schachinger E., Carbotte J.P. Gap anisotropy in superconductors with paramagnetic impurities. // J. Low Temp. Phys., 1981, vol. 42, p. 69–80.
 33. Williams P.J., Carbotte J.P. Specific heat of a d -wave superconductor stabilized by antiferromagnetic fluctuations. // Phys. Rev. B, 1989, vol. 39, p. 2180–2187.
 34. Wang N.L., Tajima S., Hauff R., Rykov A.I., Minura T. Optical study of pair-breaking effect in Zn-substituted $\text{YBa}_2\text{Cu}_3\text{O}_{7-\delta}$. // J. Chem. Phys. Solids, in print.

Обмеження на можливі механізми високотемпературної надпровідності

Е. Шахінґер, І. Шюррер

Інститут теоретичної фізики, Технічний університет м.Грац,
Петерсґассе 16, А-8010 Грац, Австрія

Отримано 23 березня 1998 р.

Дана стаття розглядає феноменологічну модель, що використовується для опису різноманітних властивостей $d_{x^2-y^2}$ надпровідників в залежності як від температури, так і від частоти, а саме глибини проникнення Лондона, оптичної провідності, мікрохвильової провідності та електронної термічної провідності. Ми вважаємо, що саме площини CuO_2 є основним чинником для виникнення надпровідності, і тому розвиваємо двомірний формалізм, в якому процеси непружного розсіяння моделюються точно через спектральну густину, що описує флуктуаційний спектр, який є відповідальним за виникнення надпровідного переходу, а також за велике непружне розсіяння, що спостерігається в нормальному стані вище критичної температури T_c . Зворотній вплив надпровідності на спектральну густину моделюється температурнозалежним низькочастотним обрізанням.

Теоретичні результати порівнюються з експериментальними даними і, виходячи з того, що дана модель дає змогу зробити послідовний опис цілого ряду явищ, формулюються обмеження на можливі механізми виникнення надпровідності в оксидах.

Ключові слова: високотемпературна надпровідність, глибина проникнення Лондона, оптична провідність, електронна теплопровідність

PACS: 74.20.Fg, 74.25.Nf, 74.72.-h

